Available online at www.sciencedirect.com
ScienceDirect
Phytochemistry 68 (2007) 2816–2824
PHYTOCHEMISTRY
www.elsevier.com/locate/phytochem

Biosynthesis of the chromogen hermidin from *Mercurialis annua* L.

Elena Ostrozhenkova [a], Eva Eylert [a], Nicholas Schramek [a], Avi Golan-Goldhirsh [b], Adelbert Bacher [a,c], Wolfgang Eisenreich [a,c,*]

[a] *Lehrstuhl für Organische Chemie und Biochemie, Technische Universität München, Lichtenbergstrasse 4, D-85747 Garching, Germany*
[b] *Ben-Gurion University of the Negev, The Jacob Blaustein Institutes for Desert Research, Albert Katz Department of Dryland Biotechnologies, Sede Boqer Campus 84990, Israel*
[c] *Ikosatec GmbH, D-85748 Garching, Germany*

Received 20 April 2007; received in revised form 25 May 2007; accepted 12 June 2007
Available online 2 August 2007

Abstract

Cut seedlings of *Mercurialis annua* L. were supplied with solutions containing 5.4 mM [U-$^{13}C_6$]glucose and 50 mM unlabelled glucose. The pyridinone type chromogen, hermidin, was isolated and analyzed by NMR spectroscopy. ^{13}C NMR spectra revealed the presence of [4,5,6-$^{13}C_3$]hermidin in significant amount. NMR analysis of amino acids obtained by hydrolysis of labelled biomass showed the presence of [U-$^{13}C_3$]alanine, whereas aspartate was found to be virtually unlabelled. Photosynthetic pulse labelling of *M. annua* plants with $^{13}CO_2$ followed by a chase period in normal air afforded [4,5,6-$^{13}C_3$]- and [2,3-$^{13}C_2$]hermidin with significant abundance. [U-$^{13}C_3$]Alanine and multiply ^{13}C-labelled aspartate isotopologues were also found in significant abundance. The labelling patterns of hermidin obtained in the present study closely resemble those observed for the pyridine ring of nicotine under similar experimental conditions. This suggests that hermidin, like nicotine, is biosynthesized *via* the nicotinic acid pathway from dihydroxyacetone phosphate and aspartate. The data show that pulse/chase labelling of plants with $^{13}CO_2$ generates isotopologue patterns that are similar to those obtained with totally labelled carbohydrate as tracer, but with the added advantage that experiments can be conducted under strictly physiological conditions. This experimental concept appears ripe for application to a wide variety of problems in plant physiology.

Keywords: Biosynthesis; NMR Spectroscopy; Hermidin; Alkaloid; Mercurialis

1. Introduction

Mercurialis annua L. (Euphorbiaceae) is an annual dioecious weed, native to the Mediterranean basin. It grows in cultivated areas and wastelands. During experiments to isolate proteins from *Mercurialis* leaves by ammonium sulphate fractionation, we noted the formation of a blue pigment in the presence of oxygen (Khadka et al., 2005). The emergence of blue coloration upon addition of ammonium carbonate to *Mercurialis* extract had already been reported by Darwin (1882). More recently, the blue material was identified as a radical anion, cyanohermidin, that is formed from hermidin by reaction with molecular oxygen (Forrester, 1984; Swan, 1984; Boger and Baldino, 1993) (Fig. 1). Cyanohermidin dimerises spontaneously into a product that is further oxidised with molecular oxygen to the yellow-brown-colored chrysohermidin (Haas and Hill, 1925; Cannan, 1926; Swan, 1985). As reported earlier by Swan (1985), hermidin is present in *Mercurialis* in relatively high concentration. Nothing appears to be known about its biosynthesis.

Metabolic pathways can be studied in plants by *in vivo* experiments using stable-isotope-labelled precursors followed by a NMR-based analysis of labelling patterns. As an example, the role of the non-mevalonate pathway for the production of numerous plant terpenoids has been established by stable isotope labelling experiments using

* Corresponding author. Address: Lehrstuhl für Organische Chemie und Biochemie, Technische Universität München, Lichtenbergstrasse 4, D-85747 Garching, Germany. Tel.: +49 89 289 13336; fax: +49 89 289 13363.
E-mail address: wolfgang.eisenreich@ch.tum.de (W. Eisenreich).

0031-9422/$ - see front matter © 2007 Elsevier Ltd. All rights reserved.
doi:10.1016/j.phytochem.2007.06.030

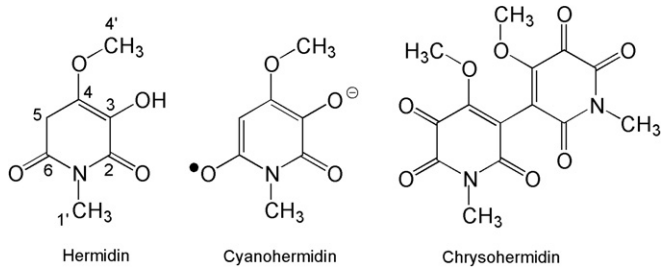

Fig. 1. Hermidin and its oxidative decomposition products (Swan, 1984; Boger and Baldino, 1993).

^{13}C-labelled glucose as a precursor (for review, see Eisenreich et al., 2004). Next to advances in NMR instrumentation, the introduction of retrobiosynthetic analysis enabled the delineation of biosynthetic pathways and flux on a quantitative basis. This approach avoids many of the pitfalls that have hampered earlier biosynthetic research with stable isotopes and is based on a detailed isotopologue analysis of certain metabolites including computational simulation of carbon partitioning (Szyperski, 1995; Bacher et al., 1999; Sauer, 2005). Specifically, starting from ^{13}C-labelled feed supplements (for example, [U-$^{13}C_6$]glucose), the distribution of label throughout the metabolic network of an organism can be monitored by quantitative NMR spectroscopy of target metabolites, such as amino acids. On the basis of established biosynthetic pathways of amino acids, their isotopologue compositions also provide the isotopologue profiles of the respective precursors (e.g., acetyl-CoA, phosphoenolpyruvate, oxaloacetate, α-ketoglutarate). Since these metabolites constitute central nodes of the metabolic network in a cell, information about fundamental metabolic fluxes can be gleaned. This paper describes labelling experiments with [U-$^{13}C_6$]glucose and pulse/chase labelling with $^{13}CO_2$ designed to analyze the biosynthesis of hermidin.

2. Results

2.1. NMR signal assignments

As a prerequisite for biosynthetic studies by ^{13}C NMR spectroscopy, all ^{13}C NMR signals of the target molecules must be unequivocally assigned. Since only ^{1}H NMR assignments for hermidin were available from the literature (Swan, 1984), the ^{13}C signals were assigned by HMQC and HMBC experiments. Moreover, multiply ^{13}C-labelled samples from the labelling experiments afforded ^{13}C^{13}C coupling constants that confirmed the assignments and were required for the subsequent biosynthetic studies. Data are summarized in Table 1.

Table 1
^{1}H and ^{13}C NMR data of hermidin

Position	Chemical shifts (ppm)		J_{CC} Coupling constants[a](Hz)	Correlation	
	^{1}H	^{13}C	^{13}C^{13}C	HMQC	HMBC
1′	3.2	26.9	–	1′	2, 6
2		165.9	73.0 (3)		OH (3)
3		122.7	73.4 (2)		OH (3), 5
4		140.1	49.1 (5)	4	3, 4′
5	3.5	35.8	50.0 (4), 50.0 (6)	5	3, 4, 6
6		167.5	50.9 (5)		1′, 5
4′	4.1	58.8	–		4
OH (3)	5.6	–	–	–	–

[a] Observed with ^{13}C-enriched samples. The coupling partner of the index carbon atom is given in parentheses.

2.2. Experiments with [U-$^{13}C_6$]glucose

Initial ^{13}C labelling studies were performed with cut seedlings of *M. annua* plants that were immersed into a solution containing 0.05% [U-$^{13}C_6$]glucose (99.9% ^{13}C enrichment) and 0.95% (w/w) unlabelled glucose. The survival of the plant material was improved considerably by the addition of ascorbic acid to the glucose solution; the vitamin is believed to act as an antioxidant that reduces damage to the cut plant material.

Hermidin was isolated from the labelled plant material as described under Section 4. The compound turned out to be highly unstable, and it was essential to run ^{13}C NMR experiments immediately after isolation.

^{13}C Signals of the hermidin sample from the experiment with [U-$^{13}C_6$]glucose are shown in Fig. 2a. The signal of C-5 comprises a central line and four satellite lines of considerable intensity that arise by ^{13}C^{13}C coupling in multiply labelled molecular species. The other ^{13}C signals appear with relatively low intensity that is due to slow relaxation in the absence of directly bound protons. Even so, satellites resulting from ^{13}C^{13}C coupling can be identified for C-4 and C-6 (Table 2).

The labelling pattern shows unequivocally that up to three ^{13}C atoms can be incorporated *en bloc* into carbon atoms 4–6 of the pyridinone ring. A more detailed analysis shows the presence of a triple-labelled as well as two different double-labelled isotopologues in the hermidin sample. The data are summarized in Fig. 3a where abundances of individual isotopologues are indicated by the width of the bars connecting jointly transferred clusters of ^{13}C atoms. Isotopologue abundances are indicated numerically in mol%.

Biomass remaining after hermidin isolation was hydrolyzed with 6 M hydrochloric acid, and alanine and aspartate from the hydrolysate were chemically converted into the tert-butyl-di-methylsilyl derivatives, respectively, that were then analyzed by mass spectrometry.

On the basis of the known fragmentation pattern of the derivative (Dauner and Sauer, 2000), isotopologue abundances can be determined for ions comprising all carbon atoms of the original amino acid (corresponding to a fragment with $m/z = 260$ from TBDMS-alanine; cf. Table 3), and for ions comprising the carbon atoms of the original

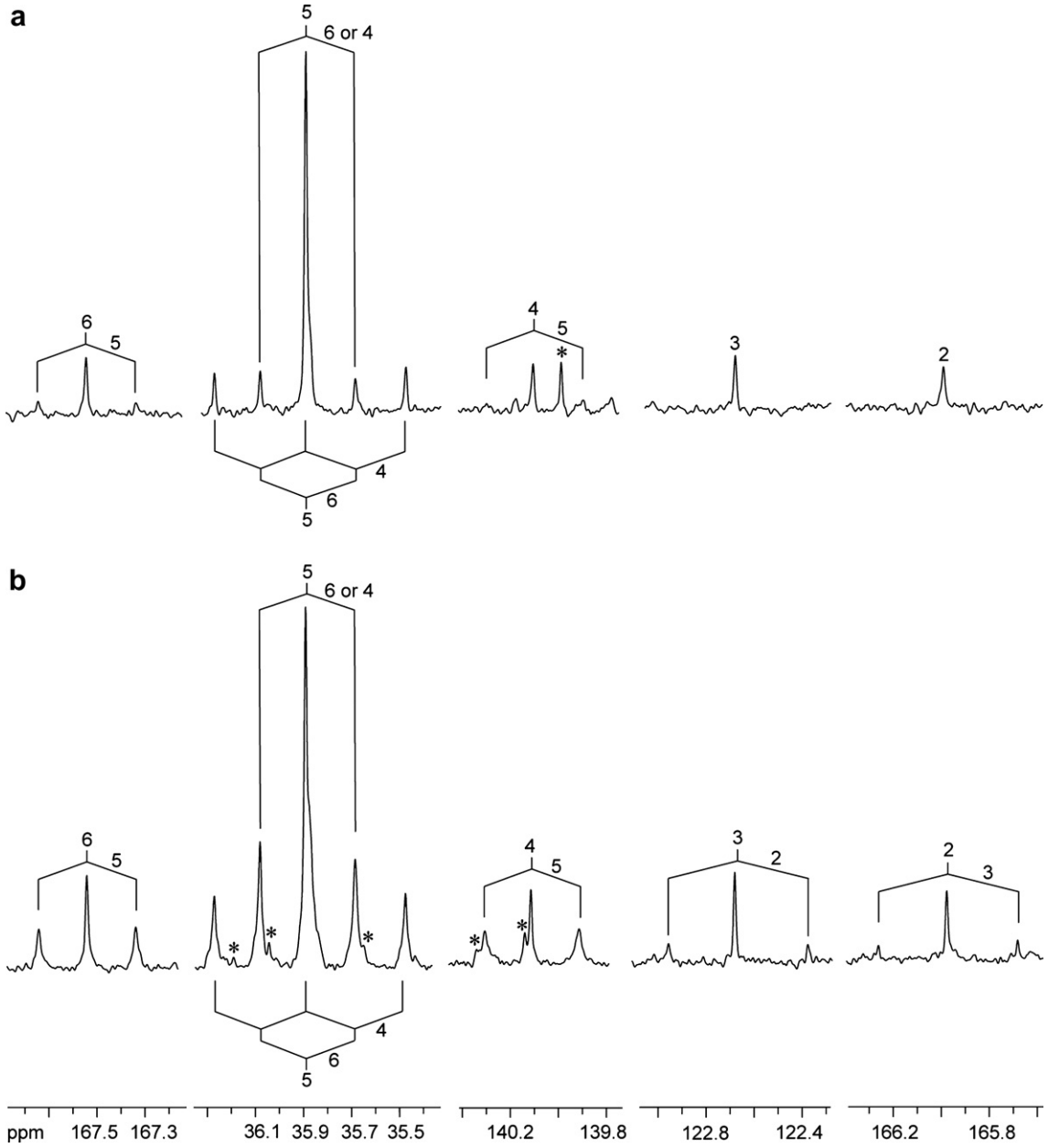

Fig. 2. ^{13}C NMR signals of hermidin from the experiments with [U-$^{13}C_6$]glucose (a) and $^{13}CO_2$ (b). Coupling patterns are indicated. The asterisks indicate signals from impurities.

amino acids without the carboxylic acid atom ($m/z = 158$ or 232 from TBDMS-alanine). After correcting the detected intensities of the mass peaks using the method described by Lee et al. (1991), molar abundances for carbon isotopologues of the amino acid moiety can be calculated (Table 3). The isotopologue pattern is derived from the abundances of isotopologue groups (*XY*-groups) as described elsewhere (Römisch-Margl et al., 2007).

The data summarized in Table 3 showed the presence of the universally labelled [U-$^{13}C_3$]alanine with an abundance of 0.6 mol%. A double-labelled [2,3-$^{13}C_2$]alanine was also detected (cf. also Fig. 4a). On the other hand, protein-derived aspartate analyzed by the same method showed no significant ^{13}C labelling.

2.3. Experiments with $^{13}CO_2$

Despite the success of the experiment with [U-$^{13}C_6$]glucose, it became clear in the course of the study that the metabolic potential of the cut plant material deteriorated rapidly during the time period required for labelling. For this reason, we decided to use $^{13}CO_2$ as tracer in a second experiment. As shown earlier, incubation of intact plants in an atmosphere containing $^{13}CO_2$ with the highest possible ^{13}C abundance affords multiply ^{13}C-labelled photosynthate (Schaefer et al., 1975, 1980; Hutchinson et al., 1976; Römisch-Margl et al., 2007). During a subsequent chase period where the plant is kept under standard greenhouse conditions, unlabelled photosynthate can be generated.

Table 2
Labelling data of hermidin from the experiment with [U-^{13}C6]glucose monitored by NMR spectroscopy

Position	%^{13}C^{13}C[a]	%^{13}C	Abundance of multiple-labelled isotopologues (mol%)
1′		<1.3	
2	–	<1.3	–
3	–	<1.3	–
4	32.4 (5)	n.d.	1.0 [4,5,6-$^{13}C_3$] + [4,5-$^{13}C_2$]
5	25.5 (4 and 6), 14.0 (4 or 6)	2.9	0.7 [4,5,6-$^{13}C_3$], 0.4 [4,5-$^{13}C_2$] + [5.6-$^{13}C_2$]
6	34.2 (5)	2.3	0.8 [4,5,6-$^{13}C_3$] + [5,6-$^{13}C_2$]
4′		1.9	

[a] Fraction (expressed as %) of ^{13}C coupled satellite signals in the overall signal integral of a given carbon atom. ^{13}C Atoms that give rise to the coupling signature are indicated in parentheses.

Catabolic fragments can then be generated from both multiply ^{13}C-labelled and unlabelled photosynthate and can be stochastically recombined by anabolic processes affording primary and secondary plant metabolites. Since the plant is not exposed to any physical damage whatsoever during the $^{13}CO_2$ pulse labelling or the subsequent chase period (in contrast to the feeding experiment with labelled glucose), its biosynthetic capacity is not compromised in any way.

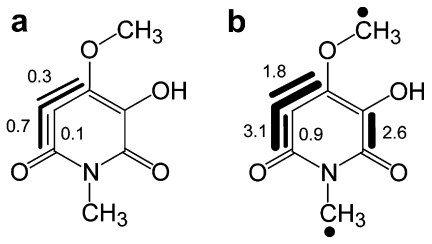

Fig. 3. (a) ^{13}C Isotopologue composition of hermidin from *M. annua* in the experiment with [U-$^{13}C_6$]glucose; (b) ^{13}C isotopologue composition of hermidin from *M. annua* in the experiment with $^{13}CO_2$. Multiple ^{13}C-labelled isotopologues are indicated by bars, single-labelled isotopologues by filled dots. The numbers indicate ^{13}C-enrichments values in mol%.

Table 3
GC/MS analysis of TBDMS-alanine

Fragment[a] (*m*/*z*)	Isotopologue/*X*-group[b]	mol (%)	SD (%)
232	{*X*00}	98.40	0.42
232 + 1	{*XYY*}^{1}	0.56	0.26
232 + 2	{*X*11}	1.04	0.25
158	{*X*00}	97.96	0.41
158 + 1	{*XYY*}^{1}	0.56	0.51
158 + 2	{*X*11}	1.48	0.10
260	{000}	90.92	4.69
260 + 1	{*YYY*}^{1}	7.69	4.73
260 + 2	{*YYY*}^{2}	0.76	0.23
260 + 3	{111}	0.63	0.25

The derivative was made from alanine obtained from protein hydrolysates of seedlings of *Mercurialis annua* labelled with [U-$^{13}C_6$]glucose.

[a] Fragment 232: loss of the tert-butyl group from the TBDMS derivate and the CO unit from the amino acid $(M-85)^+$; fragment 260: loss of the tert-butyl group from the TBDMS derivative $(M-57)^+$; fragment 158: loss of C(O)-TBDMS ion $(M-159)^+$.

[b] The *XY*-group notation of isotopologues is adapted from Römisch-Margl et al. (2007).

In the present study, we exposed *M. annua* plants to a synthetic atmosphere containing 600 ppm $^{13}CO_2$ for a period of 3 h under white light (about 20,000 lux) at a temperature of 26 °C and 66% humidity. The plants were subsequently kept in the greenhouse under standard conditions for four days. They were then harvested, and hermidin as well as biosynthetic amino acids were isolated and analyzed by NMR and mass spectrometry as described above.

Carbon NMR signals of hermidin from the $^{13}CO_2$ experiment are shown in Fig. 2b. It is immediately obvious that the relative intensity of the satellite signals indicative of multiply labelled hermidin isotopologues are generally larger in the $^{13}CO_2$ experiment as compared to the experiment with [U-$^{13}C_6$]glucose (cf. also Table 4). This appears as a direct consequence of more efficient label incorporation by the undamaged whole plants as compared to the cut plant segments. It is also obvious that the satellite patterns of carbon atoms 4–6 are similar in the two experiments. Carbon atoms 2 and 3 appear as pseudotriplets with satellites signalling the joint transfer of two ^{13}C atoms to these adjacent positions, in contrast to the experiment with the [U-$^{13}C_6$]glucose experiment where these carbon signals were devoid of apparent satellites. The isotopologue pattern deduced from the coupling patterns in the $^{13}CO_2$ experiment using published methods (Szyperski, 1995; Bacher et al., 1999; Eisenreich and Bacher, 2000; Sauer, 2005; Ettenhuber et al., 2005) are summarized in Fig. 3b. Whereas the isotopologue patterns involving carbon atoms 4–6 are qualitatively similar in the two experiments, the joint transfer of two ^{13}C atoms to positions 2 and 3 in the $^{13}CO_2$ experiment is the most notable difference between the two experiments.

The isotopologue pattern derived from the mass spectral data of biosynthetic alanine from the $^{13}CO_2$ experiment is summarized in Table 5 and Fig. 4b, and appears similar to that observed in the labelling experiment with [U-$^{13}C_6$]glucose, except that the amino acid from the $^{13}CO_2$ experiment shows a higher level of label, in line with the observed isotopologue pattern of hermidin. Several multiply ^{13}C-labelled aspartate isotopologues were detected at significant abundance (Table 6 and Fig. 4b), whereas aspartate had been found to be virtually without label in the experiment with [U-$^{13}C_6$]glucose.

3. Discussion

Tracer studies with stable and radioactive isotopes are powerful instruments for the study of biosynthesis and metabolite flux. A variety of methods are available for the application of isotope-labelled tracer compounds in studies with plants. (i) Aqueous tracer solutions can be fed to cut plant segments. (ii) Certain tracers such as isotope-labelled glucose can be applied *via* the root system

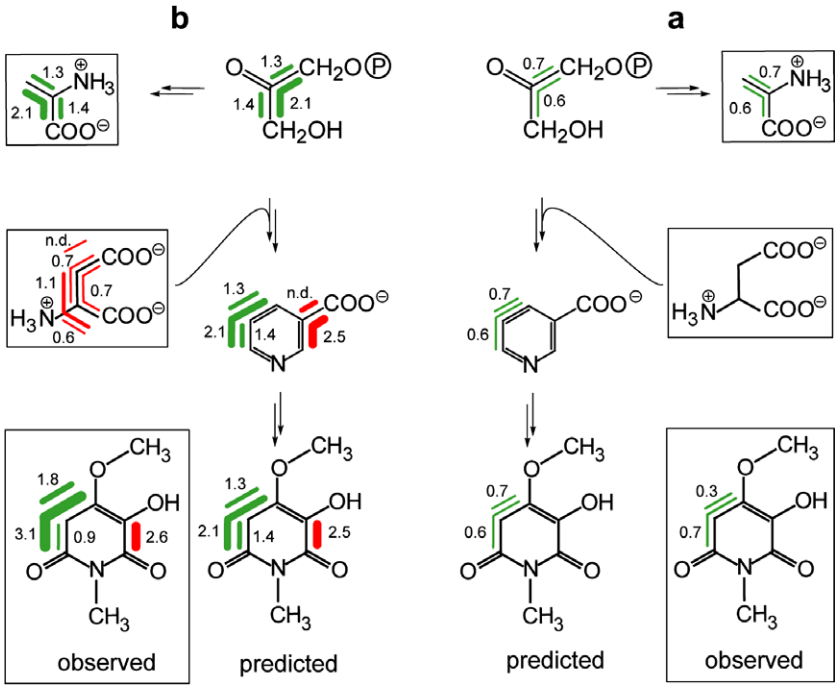

Fig. 4. Comparison of the labelling patterns in hermidin observed by quantitative NMR spectroscopy with predicted patterns *via* the aspartate route of nicotinic acid biosynthesis. The prediction is based on the observed profiles in alanine and aspartate (shown in boxes). For details see Section 2 and legend to Fig. 3.

Table 4
Labelling data of hermidin from the $^{13}CO_2$ experiment monitored by NMR spectroscopy

Position	$\%^{13}C^{13}C$[a]	$\%^{13}C$	Abundance of multiple-labelled isotopologues (mol%)
1′		5.4	
2	35.0 (3)	7.4	2.6 [2,3-$^{13}C_2$]
3	38.3 (2)	7.0	2.7 [2,3-$^{13}C_2$]
4	60.6 (5)	8.0	4.9 [4,5,6-$^{13}C_3$] + [4,5-$^{13}C_2$]
5	39.2 (4 and 6), 32.5 (4 or 6)	7.9	3.1 [4,5,6-$^{13}C_3$], 2.6 [4,5-$^{13}C_2$] + [5,6-$^{13}C_2$]
6	54.1 (5)	7.7	4.2 [4,5,6-$^{13}C_3$] + [5,6-$^{13}C_2$]
4′		6.6	

[a] Fraction of ^{13}C coupled satellite signals in the overall signal integral of a given carbon atom. ^{13}C Atoms that give rise to the coupling signature are indicated in parentheses.

Table 5
GC/MS analysis of TBDMS-alanine

Fragment (*m/z*)	Isotopologue/*X*-group	mol (%)	SD (%)
232	{*X*00}	92.59	0.22
232 + 1	{*XYY*}[1]	3.81	0.03
232 + 2	{*X*11}	3.60	0.18
158	{*X*00}	92.86	0.21
158 + 1	{*XYY*}[1]	3.70	0.25
158 + 2	{*X*11}	3.44	0.22
260	{000}	85.74	1.55
260 + 1	{*YYY*}[1]	9.39	1.58
260 + 2	{*YYY*}[2]	2.73	0.06
260 + 3	{111}	2.14	0.11

The derivative was made from alanine obtained from protein hydrolysates of leaves of *Mercurialis annua*. The leaves were cut from plants grown in the presence of $^{13}CO_2$. For more details, see also footnotes of Table 3.

of plants that have been grown under aseptic conditions. (iii) Cultured plant cells can be grown in medium containing the tracer.

Each of these methods has specific shortcomings. The use of cut segments involves traumatization of the plant tissue followed by rapid functional decline. Aseptically grown plants and/or tissue cultures are available for certain plant species but not for others. Moreover, cultured plant cells tend to loose biosynthetic potential and may display metabolic alterations by comparison with whole plants.

By comparison with these techniques, the use of $^{13}CO_2$ as tracer is atraumatic. Labelling experiments can be performed with whole plants under a wide variety of experimental conditions, and the extent of labelling can be modulated over a relatively wide range *via* the experimental conditions of the $^{13}CO_2$ pulse and the length of a consecutive chase period in normal air.

$^{14}CO_2$ Labelling was a fundamental tool in the pioneering studies on photosynthesis by Calvin, Bassham and their coworkers (for review, see Bassham, 2003). On the other hand, there are hitherto few examples for the use of $^{13}CO_2$ as tracer in plant physiology (Schaefer et al., 1975, 1980; Hutchinson et al., 1976; Römisch-Margl et al., 2007). The technology is based on the concept that a pool of multiply labelled photosynthate, predominantly in the form of monomeric and polymeric hexose derivatives, can be generated in an atmosphere of synthetic air containing highly enriched $^{13}CO_2$. Catabolic processing of these second generation tracer compounds (second generation by comparison with the applied $^{13}CO_2$) can afford a variety

Table 6
GC/MS analysis of TBDMS-aspartate obtained from protein hydrolysates of leaves of *Mercurialis annua*

Fragment[a] (*m*/*z*)	Isotopologue/*X*-group	mol (%)	SD (%)
302	{00*XX*}	93.90	0.17
302 + 1	{*YYXX*}[1]	3.76	0.10
302 + 2	{11*XX*}	2.34	0.11
316	{*X*000}	91.08	0.33
316 + 1	{*XYYY*}[1]	5.02	0.17
316 + 2	{*XYYY*}[2]	2.79	0.15
316 + 3	{*X*111}	1.11	0.05
390	{*X*000}	91.52	0.39
390 + 1	{*XYYY*}[1]	5.60	0.15
390 + 2	{*XYYY*}[2]	1.49	0.74
390 + 3	{*X*111}	1.39	0.39
418	{0000}	89.51	0.25
418 + 1	{*YYYY*}[1]	4.85	0.22
418 + 2	{*YYYY*}[2]	3.10	0.28
418 + 3	{*YYYY*}[3]	1.84	0.20
418 + 4	{1111}	0.71	0.09

The leaves were cut from plants grown in the presence of $^{13}CO_2$.

[a] Fragment 390: loss of the tert-butyl group from the TBDMS derivate and the CO unit from the amino acid $(M-85)^+$; fragment 418: loss of the tert-butyl group from the TBDMS derivative $(M-57)^+$; fragment 316: loss of C(O)-TBDMS ion $(M-159)^+$; fragment 302: double silylated C_1–C_2 fragment $(302)^+$.

of multiply labelled third generation metabolites which can then be combined by anabolic processes with molecular species derived from unlabelled biomass. As a result, one can expect the formation of metabolites which can be interpreted as molecular mosaics assembled at random from labelled as well as unlabelled precursors. In the final outcome, the labelling patterns of the anabolites resulting from these processes may be similar to the patterns expected for experiments with multiply labelled carbohydrate tracers such as [U-$^{13}C_6$]glucose.

In order to test this prediction, we have previously conducted labelling experiments with tobacco using either $^{13}CO_2$ (Römisch-Margl et al., 2007) or [U-$^{13}C_6$]glucose (unpublished data) as tracer. As summarized in Fig. 5, the labelling patterns of nicotine observed in these experiments were similar. It should be noted that these experiments were conducted to check the method and not the biosynthetic pathway of nicotine, which was already known in considerable detail (for reviews, see Leete, 1992; Bush et al., 1999; Katoh and Hashimoto, 2004).

In the present paper, we conducted a similar side by side study using $^{13}CO_2$ and [U-$^{13}C_6$]glucose, in order to analyze the biosynthesis of hermidin, which was previously unknown. In close parallel with the tobacco experiments, we found that the labelling patterns generated by the two different labelling strategies are similar (Fig. 5). Notably, the ^{13}C abundance is considerably lower in the experiment with ^{13}C-labelled glucose, and that can be explained by the fact that the tissue segments undergo rapid attrition. However, both experiments unequivocally show the diversion of up to three ^{13}C atoms in tandem to carbon atoms 4–6 of hermidin. Significant pairwise incorporation of adjacent ^{13}C atoms into carbon atoms 2 and 3 was only observed

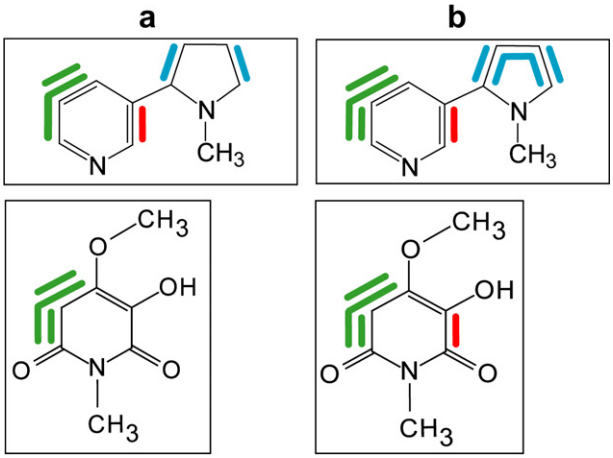

Fig. 5. Comparison of labelling patterns in hermidin and nicotine from the [U-$^{13}C_6$]glucose experiment (a) and the $^{13}CO_2$ experiment (b). The bars indicate multiple-labelled isotopologues. Due to the different scaling factors the labelling patterns are shown only qualitatively. The nicotine pattern from the $^{13}CO_2$ experiment is published in Römisch-Margl et al., 2007. The pattern from the [U-$^{13}C_6$]glucose experiment is unpublished.

in case of the $^{13}CO_2$ experiment, but this difference may be due to the generally low transfer of label in the experiment with labelled glucose.

It cannot escape notice that the labelling patterns of the pyridine ring in nicotine (in earlier experiments with tobacco) and the pyridinone ring of hermidin (in the present experiments) are similar. In light of the known origin of the pyridine ring of nicotine from the nicotinic acid biosynthetic pathway, this prompts the hypothesis that hermidin is also derived from the nicotinic acid pathway (i.e. either from nicotinic acid or a nicotinic acid precursor). The plausibility of this hypothesis can be checked still further by comparison of the labelling patterns of the secondary metabolites under study (i.e. nicotine and hermidin) with those of primary metabolites such as amino acids.

Nicotinic acid biosynthesis in plants is assumed to start from dihydroxyacetone phosphate and iminoaspartate (derived from aspartate by aspartate oxidase, NadB protein, cf. Fig. 6) which undergo a condensation affording quinolinate catalysed by quinolinate synthase (NadA protein) (Fig. 6) (for review, see Noctor et al., 2006). Using the experimentally determined labelling patterns of the amino acids from the experiments with $^{13}CO_2$ or [U-$^{13}C_6$]glucose as tracers, the labelling patterns of hermidin can be simulated using the retrobiosynthetic concept[1]

[1] *Definition of retrobiosynthetic analysis*: Reconstruction of the labelling patterns of central metabolic intermediates (e.g. acetyl-CoA, triose phosphates, oxaloacetate, 2-ketoglutarate) on the basis of known biosynthetic routes leading to the labelling patterns in sink metabolic products, such as amino acids, fatty acids or storage carbohydrates. The reconstructed patterns are then used to predict hypothetical labelling patterns in a complex biosynthetic product (e.g. a secondary metabolite) by a given biosynthetic pathway. The concept was introduced in analogy to the retro-concept in synthetic organic chemistry, where possible precursors are reconstructed from the structure of a desired synthetic product.

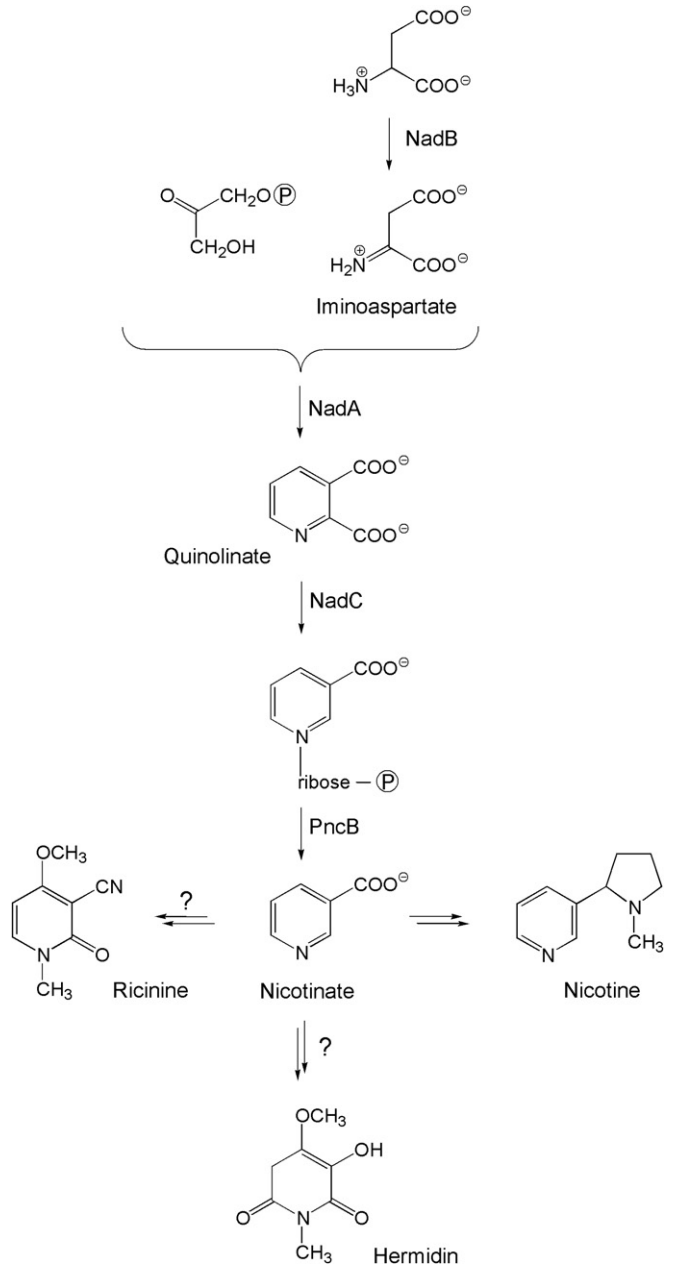

Fig. 6. Hypothetical biosynthetic pathway of nicotinic acid and downstream products in plants (for review, see, Noctor et al., 2006).

that we have pioneered for the unravelling of biosynthetic pathways (Bacher et al., 1999). The retrobiosynthetic reconstruction agrees well with the experimentally observed labelling patterns of hermidin (Fig. 4). Notably, aspartate from the $^{13}CO_2$ experiment shows multiply labelled isotopologues in significant abundance, whereas these isotopologues are below the detection limit in the experiment with [U-$^{13}C_6$]glucose. This finding corresponds very well with the presence of [2,3-$^{13}C_2$]hermidin in the sample from $^{13}CO_2$ labelling and its absence in the sample from [U-$^{13}C_6$]glucose labelling.

The absence of labelling in aspartate in the labelling experiment with [U-$^{13}C_6$]glucose may reflect the breakdown of aspartate biosynthesis under the experimental conditions. As noted above, cut segments of *M. annua* showed signs of tissue damage. Alternatively, the failure to label aspartate from [U-$^{13}C_6$]glucose could be linked to discontinuation of aspartate/asparagine supply from the roots in the experiment with the cut seedlings. Since the plants used in the $^{13}CO_2$ were not exposed to any physical or chemical damage, it comes as no surprise that all biosynthetic pathways remain fully operative throughout the experiment, with consecutive diversion of ^{13}C to all metabolic compartments.

Our earlier work on the formation of nicotine in intact tobacco plants has already shown that similar labelling patterns of amino acids and of nicotine emerged in experiments with [U-$^{13}C_6$]glucose (that was supplied *via* the roots of aseptically grown tobacco plants) (unpublished data) and in pulse/chase experiments with $^{13}CO_2$ (Römisch-Margl et al., 2007). The results of the present study present further support for the hypothesis that the pulse/chase experiment with $^{13}CO_2$ can be considered as an equivalent of [U-$^{13}C_6$]glucose feeding. This is not surprising since hexose phosphates are a main product of photosynthesis, which can be stored as starch for later reutilization during dark periods.

We suggest that pulse/chase labelling with $^{13}CO_2$ can be utilized for a wide variety of experiments directed at the study of biosynthesis and metabolic flux in plants. Advanced NMR spectroscopy and mass spectrometry enable the delineation of complex isotopologue mixtures generated in $^{13}CO_2$ experiments. On this basis, metabolic pathways can be identified and quantified with high resolution. Most notably, the plants undergo no mechanical interference or damage, the labelling experiments can be performed with plants grown under standard conditions (as opposed to the use of aseptic plants for the application of labels *via* the root system), and the experiments can be conducted under greenhouse or even field conditions were required.

4. Experimental

4.1. Plants

Seedlings of *M. annua* L. were grown in the greenhouse using commercial gardening soil mixture (Terreau Professional Gepac Einheits Erde, Germany). The growth conditions were: 14 h light per day; day temperature, 25–28 °C; night temperature, 20–23 °C; relative humidity, 50%. Six to eight weeks old seedlings were used for the labelling experiments.

4.2. Chemicals

[U-$^{13}C_6$]Glucose (99% ^{13}C abundance) was obtained from Sigma–Aldrich, and $^{13}CO_2$ (>99% ^{13}C abundance) was purchased from Campro Scientific, Berlin, Germany.

4.3. $^{13}CO_2$ labelling

Growing plants of *M. annua* with a height of about 20 cm were placed in a plant growth chamber (BIOBOX, GWS, Berlin). During an adaption light period of 6 h at 26 °C and a light period of 12 h at 22 °C and 66% humidity, the plants were exposed to synthetic air containing 20.5% oxygen and 600 ppm CO_2. The chamber was flushed with an oxygen/nitrogen mixture (20:80, v/v), and the plants were then exposed to synthetic air containing 600 ppm $^{13}CO_2$ under white light (20,000 lux) at 26 °C for 3 h. Subsequently, the plants were kept in the dark for 18 h and were then allowed to grow under standard greenhouse conditions at ambient temperature for four days.

4.4. Labelling experiments with [U-$^{13}C_6$]glucose

Five cut seedlings of *M. annua* (approximately 15 g, fresh weight) were immersed in a solution containing 0.05% [U-$^{13}C_6$]glucose (99.9% ^{13}C enrichment), 0.95% (w/w) unlabelled glucose and 1 mM ascorbic acid. Each cut seedling was incubated in the dark for five days in separate flasks each containing about 10 ml of the solution. If required, solution was added to the flasks. The seedlings consumed approximately 100 ml of the solution.

4.5. Isolation of hermidin

Plant material (fresh weight, 15 g) was triturated with liquid nitrogen. To the cold slurry, 150 ml of distilled water and 5 ml of chloroform were added, and the mixture was kept under a nitrogen atmosphere for 45 min. The slurry was filtered, and sodium dithionite (500 mg) was added. The mixture was extracted with two 100 ml portions of chloroform. The organic phase was evaporated to dryness under reduced pressure.

4.6. Protein hydrolysis and amino acid derivatization

Freeze-dried plant material (100 mg) was suspended in 2 ml of 6 M hydrochloric acid. The mixture was heated at 105 °C for 24 h under an inert atmosphere and was then centrifuged. An aliquot (500 μl) of the supernatant was dried under a stream of nitrogen. The residue was dissolved in 50 μl of acetonitrile. *N*-(tert-butyldimethylsilyl)-*N*-methyl-trifluoroacetamide containing 1% tert-butyldimethyl-silylchloride (50 μl) was added. The mixture was kept at 70 °C for 30 min and was used for GC/MS analysis without further work-up.

4.7. NMR spectroscopy

NMR spectra were recorded at 27 °C using a DRX 500 spectrometer (Bruker Instruments, Karlsruhe, Germany). Hermidin was measured in $CDCl_3$ as solvent. Two-dimensional COSY, HMQC, HMBC experiments were measured with standard Bruker software (TopSpin).

4.8. Isotopologue abundances by NMR spectroscopy

Relative ^{13}C abundance was determined by comparing the signal intensities of the biosynthetic samples with the signals of samples with natural ^{13}C abundance measured under identical spectroscopic conditions (Eisenreich and Bacher, 2000). Absolute ^{13}C abundances of individual isotopologues were determined as described earlier (Eisenreich and Bacher, 2000).

4.9. Mass spectrometry

GC/MS analysis was performed using a GC-17A Gas Chromatograph (Shimadzu, Duisburg, Germany) equipped with a fused silica capillary column (Equity TM-5; 30 m × 0.25 mm × 0.25 μm film thickness; SUPELCO, Bellafonte, PA) and a QP-5000 mass selective detector (Shimadzu, Duisburg, Germany) working with electron impact ionization at 70 eV. An aliquot (1 μl) of a solution containing TBDMS amino acids was injected in 1:5 split mode (interface temperature, 260 °C; helium inlet pressure, 70 kPa). The column was developed at 150 °C for 3 min and then with a temperature gradient of 7 °C/min to a final temperature of 280 °C that was held for 3 min. Data were collected using the Class 5000 software (Shimadzu, Duisburg, Germany). Selected ion monitoring experiments were carried out on the fragments summarized in Tables 3, 5 and 6 (for details, see also Römisch-Margl et al., 2007). Selected ion monitoring data were acquired using a 0.3 s sampling rate. Samples were analyzed at least three times.

4.10. Isotopologue abundances by GC/MS

Data evaluation was performed using Microsoft Excel Software. Theoretical isotope ratio and numerical deconvolution of the data were computed according to Lee et al. (1991) resulting in molar excess of carbon isotopologue groups (*X*-groups) or isotopologues of the amino acid skeleton.

Acknowledgements

This work was supported by a grant from the Hans Fischer Gesellschaft. We thank Prof. Peter Schröder (GSF Munich) for support and discussions and Fritz Wendling for expert technical assistance.

References

Bacher, A., Rieder, C., Eichinger, D., Fuchs, G., Arigoni, D., Eisenreich, W., 1999. Elucidation of biosynthetic pathways and metabolic flux patterns via retrobiosynthetic NMR analysis. FEMS Microbiol. Rev. 22, 567–598.

Bassham, J.A., 2003. Mapping the carbon reduction cycle: a personal retrospective. Photosynth. Res. 76, 35–52.

Boger, D.L., Baldino, C.M., 1993. *d,l*- and *meso*-isochrysohermidin: total synthesis and interstrand DNA cross-linking. J. Am. Chem. Soc. 115, 11418–11425.

Bush, L., Hempfling, W.P., Burton, H., 1999. Biosynthesis of nicotine and related compounds. In: Gorrod, J. (Ed.), Analytical Determination of Nicotine and Related Compounds and their Metabolites. Elsevier, Amsterdam, pp. 13–44.

Cannan, R.K., 1926. Electrode potentials of hermidin, the chromogen of *Mercurialis perennis*. Biochem. J. 20, 927–937.

Darwin, C.R., 1882. The action of carbonate of ammonia on the roots of certain plants. J. Linnean Soc. London (Botany) 19, 239–261.

Dauner, M., Sauer, U., 2000. GC–MS analysis of amino acids rapidly provides rich information for isotopomer balancing. Biotechnol. Progr. 16, 642–649.

Eisenreich, W., Bacher, A., 2000. Elucidation of biosynthetic pathways by retrodictive/predictive comparison of isotopomer patterns determined by NMR spectroscopy. In: Setlow, J.K. (Ed.), Genetic Engineering, Principles and Methods, vol. 22. Kluwer Academic/Plenum Publishers, New York, pp. 121–153.

Eisenreich, W., Bacher, A., Arigoni, D., Rohdich, F., 2004. Biosynthesis of isoprenoids via the non-mevalonate pathway. Cell. Mol. Life Sci. 61, 1401–1426.

Ettenhuber, C., Radykewicz, T., Kofer, W., Koop, H.U., Bacher, A., Eisenreich, W., 2005. Metabolic flux analysis in complex isotopomer space. Recycling of glucose in tobacco plants. Phytochemistry 66, 323–335.

Forrester, A.R., 1984. Autoxidation of hermidin: an ESR study. Experientia 40, 688–689.

Haas, P., Hill, T.G., 1925. *Mercurialis*. III. A consideration of the physiological significance of the chromogen. Ann. Bot. 39, 861–865.

Hutchinson, C.R., Hsia, M.T., Stephen, C.R.A., 1976. Biosynthetic studies with carbon-13 dioxide of secondary plant metabolites. *Nicotiana* alkaloids. 1. Initial experiments. J. Am. Chem. Soc. 98, 6006–6011.

Katoh, A., Hashimoto, T., 2004. Molecular biology of pyridine nucleotide and nicotine biosynthesis. Front. Biosci. 9, 1577–1586.

Khadka, D.K., Nejidat, A., Tal, M., Golan-Goldhirsh, A., 2005. Molecular characterization of a gender-linked DNA marker and a related gene in *Mercurialis annua* L. Planta 222, 1063–1070.

Lee, W.N., Byerley, L.O., Bergner, E.A., Edmond, J., 1991. Mass isotopomer analysis: theoretical and practical considerations. Biol. Mass Spectrom. 20, 451–458.

Leete, E., 1992. The biosynthesis of nicotine and related alkaloids in intact plants, isolated plant parts, tissue cultures, and cell-free systems. Environ. Sci. Res. 44, 121–139 (Secondary-Metabolite Biosynthesis and Metabolism).

Noctor, G., Queval, G., Gakière, B., 2006. NAD(P) synthesis and pyridine nucleotide cycling in plants and their potential importance in stress conditions. J. Exp. Bot. 57, 1603–1620.

Römisch-Margl, W., Schramek, N., Radykewicz, T., Ettenhuber, C., Eylert, E., Huber, C., et al., 2007. $^{13}CO_2$ as a universal metabolic tracer in isotopologue perturbation experiments. Phytochemistry, in press. doi:10.1016/j.phytochem.2007.06.030.

Sauer, U., 2005. Metabolic flux analysis: a key methodology for systems biology of metabolism. Top. Curr. Genet. 13, 191–214.

Schaefer, J., Stejskal, E.O., Beard, C.F., 1975. Carbon-13 nuclear magnetic resonance analysis of metabolism in soybeans labeled by $^{13}CO_2$. Plant Physiol. 55, 1048–1053.

Schaefer, J., Kier, L.D., Stejskal, O.E., 1980. Characterization of photorespiration in intact leaves using carbon-13 carbon dioxide labeling. Plant Physiol. 65, 254–259.

Swan, G.A., 1984. Hermidin, a chromogen from *Mercurialis perennis* L. Experientia 40 (7), 687–688.

Swan, G.A., 1985. Isolation, structure, and synthesis of hermidin, a chromogen from *Mercurialis perennis* L. J. Chem. Soc., Perkin Trans. 8, 1757–1766.

Szyperski, T., 1995. Biosynthetically directed fractional ^{13}C-labeling of proteinogenic amino acids. An efficient analytical tool to investigate intermediary metabolism. Eur. J. Biochem. 232, 433–448.